ELSEVIER

Journal of Organometallic Chemistry 518 (1996) 29–36

Journal of Organometallic Chemistry

Synthesis and NMR structural analysis of several orthopalladated complexes of substituted benzo-imidazole, -oxazole and -thiazole and study of two polymorphic crystals

Carmen Navarro-Ranninger [a,*], Félix Zamora [a], L. Alfonso Martínez-Cruz [b], Raul Isea [b], José R. Masaguer [a]

[a] *Departamento de Química Inorgánica, Facultad de Ciencias, Universidad Autónoma de Madrid, 28049 Madrid, Spain*
[b] *Departamento de Cristalografía, Instituto Rocasolano-CSIC, Serrano 119, 28006 Madrid, Spain*

Received 20 October 1995

Abstract

The full assignation of ^{1}H and ^{13}C NMR parameters using both homo- and hetero-nuclear two dimensional spectroscopy techniques (COSY, HMQC and HMBC) allows the determination of electronic properties in cyclopalladated complexes obtained by reaction of *N*-methyl-2-phenylbenzimidazole (**a**), 2-phenylbenzothiazole (**b**) and 2-phenylbenzoxazole (**c**) with palladium salts.

The attempts to separate the anti and syn isomers (detected by NMR) led to the formation of two different kinds of crystal for the 2-phenylbenzoxazole palladium complex, **1c** (yellow and orange). The X-ray diffraction study of these crystals indicates the formation of two polymorphic phases both in anti disposition.

Keywords: Palladium; Orthopalladation; X-ray structure; NMR; Synthesis

1. Introduction

Cyclometalated complexes have been intensively studied in recent years [1]. The variation of specific ^{1}H and ^{13}C NMR signals are sometimes used to confirm metalation. However, to determine valuable characteristics of orthometalated complexes such as the presence of syn–anti isomers [2,3] and electronic properties of the metalacycle [4] it is necessary to achieve an unambiguous assignation of all NMR signals corresponding to carbons and protons of the compounds [5,6].

Although Churchill et al. had determined the crystal structures of the acetate dimers derived from 2-*p*-tolylphenylbenzothiazole and 2-*p*-tolylphenylbenzoxazole [7], we thought that the ligands, *N*-methyl-2-phenylbenzimidazole (**a**), 2-phenylbenzothiazole (**b**), and 2-phenylbenzoxazole (**c**), with three different heteroatoms (N, O and S) could be interesting for studying the characteristics of the cyclometalated ring, the possible formation and isolation of anti and syn isomers, and the full assignation of protons and carbons (inclusive quaternaries not assigned in previous work [6]) by NMR techniques. We have determined the ^{1}H and ^{13}C NMR parameters using both homo- and hetero-nuclear two dimensional correlation spectroscopy (COSY, HMQC [8] and HMBC [9]). We have obtained two polymorphic crystals of the anti isomer (analysed by X-ray diffraction) in trying to crystallize anti and syn isomers detected by ^{1}H-NMR.

2. Results and discussion

A schematic representation of the routes used for the synthesis of complexes is given in Fig. 1. The best yields in these reactions were obtained for the conditions outlined in the experimental section.

The IR spectra of **1a–c** show two strong bands at ca. 1570 and 1415 cm^{-1} corresponding to $\nu_{as}(COO)$ and $\nu_{s}(COO)$ stretching vibrations of the acetate bridge respectively [10].

The MS-FAB spectra taking account of the distribution of palladium isotopes show peaks m/z at 746.2,

* Corresponding author.

Elsevier Science S.A.
PII S002-328X(96)06218-3

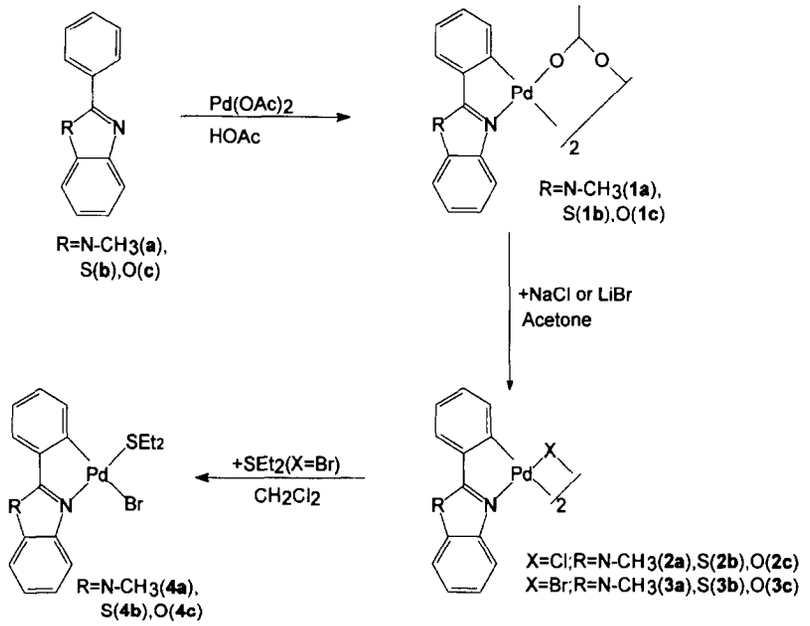

Fig. 1. Scheme of the synthetic routes.

752.0 and 719.9 assigned to the molecular ions $[M^+]$ **1a**, **1b** and **1c** respectively. Peaks corresponding to $[M^+ - OAc]$ are observed at m/z 687.2, 693.0 and 661.1.

The IR of **2a–c** showed two ν_{as}(Pd–Cl) bands at ca. 333–312 and 279–294 cm^{-1}. On the basis of the higher trans influence of a carbon atom compared with that of a nitrogen atom, the higher frequency band was attributed to the stretching vibration ν_{as}(Pd–Cl) trans to the nitrogen atom and the lower frequency one to ν_{as}(Pd–Cl) trans to the σ-bonded carbon [11].

MS-FAB spectra of complexes **3a** and **3c** showed peaks at m/z 793.7 and 761.8. The peaks at 712.8 and 680.9 were assigned to molecular ions $[M^+]$ and $[M^+ - Br]$.

Diethylsuphide monomeric compounds, **4a–c**, were obtained from μ-bromo complexes, **3a–c**. When reactions were carried out with the analogous chloro complexes no reaction was observed. Therefore, the Pd–Br bond appears to be more reactive than the Pd–Cl bond.

In the MS-FAB spectra of complex **4b** (it was not possible to record MS-FAB spectra of **4a** and **4c** since they show decomposition) the peak of higher m/z at 761.8 correspond to the bridged bromo complex **3b**, probably formed by decomposition of **4b** under MS-FAB conditions [12].

2.1. NMR studies

Unambiguous assignation of NMR parameters in the phenyl ring of the orthopalladated complexes was done on the basis of HMQC, HMBC and COSY experiments.

Table 1
Selected bond distances (Å)

1c-*orange*					
Pd1–Pd2	2.849(1)	N2–C201	1.32(2)	C301–C308	1.40(2)
Pd1–C109	2.00(1)	C201–C208	1.39(2)	C308–C309	1.45(2)
Pd1–N1	1.99(1)	C208–C209	1.42(2)	Pd4–C409	1.99(1)
N1–C101	1.37(2)	Pd3–Pd4	2.855(1)	Pd4–N4	1.997(9)
C101–C108	1.39(2)	Pd3–C309	1.93(1)	N4–C401	1.33(2)
C108–C109	1.38(2)	Pd3–N3	2.037(9)	C401–C408	1.41(2)
Pd2–C209	1.97(1)	N3–C301	1.32(1)	C408–C409	1.40(2)
Pd2–N2	2.04(1)				
1c-*yellow*					
Pd1–Pd2	2.831(3)	C101–C108	1.42(4)	N2–C201	1.26(5)
Pd1–C109	1.98(3)	C108–C109	1.38(5)	C201–C208	1.45(4)
Pd1–N1	2.02(2)	Pd2–C209	2.04(5)	C208–C209	1.38(5)
N1–C101	1.29(3)	Pd2–N2	2.04(2)		

Table 2
^{1}H NMR parameters (δ, ppm)

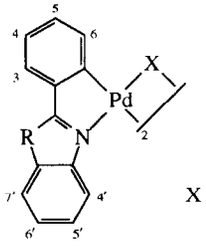

X = O(CH$_3$)O (**1a–1c**), Br (**3a**, **3c**)

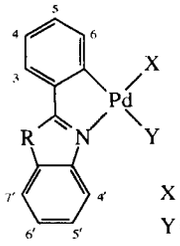

X = S(Et)–CH$_2$–CH$_3$

Y = Br (**4a–4c**)

	a [b]	**b** [b]	**c** [b]	**1a** [b,f]	**1b** [b,f]	**1c** [b,f]	**3a** [a]	**3c** [a]	**4a** [b]	**4b** [b]	**4c** [b]
H3	7.74, m, 2H	8.10, m, 2H	8.24, m, 2H	6.97, dd, 1H J = 1.2, 7.7	6.85, dd, 1H J = 1.2, 7.5	7.04, dd, 1H J = 1.2, 7.5	7.76, m, 1H	7.55, m [c]	7.63, m, 1H	7.54, m [c]	7.66, dd, 1H J = 1.7, 7.3
H4	7.50, m [c]	7.49, m [c]	7.51, m [c]	6.52, dt, 1H J = 1.2, 7.5	6.41, dt, 1H J = 1.2, 7.7	6.55, dt, 1H J = 1.2, 7.7	7.14, m, 1H	7.12, t-b, 1H J = 7.0	7.18, m [c]	7.20, m [c]	7.23, dt, 1H J = 1.2, 7.3
H5	7.50, m [c]	7.49, m [c]	7.51, m [c]	5.92, dt, 1H J = 1.2, 7.7	6.16, dt, 1H J = 1.2, 7.5	6.20, dt, 1H J = 1.2, 7.5	7.00, m, 1H	7.00, m, 1H	7.18, m [c]	7.20, m [c]	7.29, dt, 1H J = 1.8, 7.3
H6	(see H4)	(see H4)	(see H4)	6.42, dd, 1H J = 1.2, 7.5	6.55, dd J = 1.2, 7.7	6.58, dd, 1H J = 1.2, 7.7	8.07, m, 1H	8.01, d-b, 1H J = 7.8	7.78, m, 1H	7.71, m, 1H	7.69, dd, 1H J = 1.8, 7.3
H4′	7.84, m, 1H	8.08, m, 1H	7.76, m, 1H	7.51, m, 1H	7.90, td, 1H J = 0.7, 7.6	7.35, m, 1H	7.75, m, 1H	8.63, m, 1H	9.20, m, 1H	9.75, d-b, 1H J = 8.7	8.91, dd, 1H 2.0, 6.9
H5′	7.30, m [c]	7.49, m [c]	7.33, m [c]	7.19, m [c]	7.26, m [c]	7.30, m [c]	7.31, m [c]	7.55, m [c]	7.30, m [c]	7.54, m [c]	7.39, m [c]
H6′	7.30, m [c]	7.38, m, 1H	7.33, m [c]	7.19, m [c]	7.26, m [c]	7.30, m [c]	7.31, m [c]	7.48, m, 1H	7.30, m [c]	7.40, m, 1H	7.39, m [c]
H7′	7.30, m [c]	7.90, m, 1H	7.73, m, 1H	7.02, m, 1H	7.47, td, 1H J = 0.7, 8	7.30, m [c]	7.31, m [c]	8.18, d-b J = 7.7	7.30, m [c]	7.80, m, 1H	7.57, m, 1H
H8′			2.31, s, 3H [d]	2.32, s, 3H [d]	2.33, s, 3H [d]						
				2.29, s [e]	2.28, s [e]	2.30, s [e]					
				2.36, s [e]	2.39, s [e]	2.39, s [e]					
H10′									2.55, s-b, 2H	3.00, s-b, 2H	3.00, s-b, 2H
H11′									1.46, m, 3H	1.44, m, 3H	1.48, t, 3H J = 7.5
CH$_3$	3.79, s, 3H			3.68, s, 3H [d]			4.19, s, 3H		4.10, s, 3H		
				3.63, s [e]							

[a] DMSO-d_6. [b] $CDCl_3$. [c] Overlapped signal. s, singlet; d, doublet; t, triplet; m, multiplet; b, broad. J (Hz). [d] *anti* isomer. [e] *syn* isomer. [f] Other overlapped and weak aromatic signals appeared corresponding to the *syn* isomer.

The complex **1c** was selected to describe an example of the general method applied to assign NMR parameters since we have additionally studied its structure by X-ray diffraction. HMBC experiment allows the assignation of C1′ as long as it is the unique quaternary carbon connected to only one phenyl proton. The carbon at 170.0 ppm is connected to only one proton at 7.04 ppm (Fig. 2). Therefore, the signal at 7.04 ppm is assigned to H3 (C3 is assigned by HMQC) and the signal at 170.0 ppm to C1′. Also, H3 is connected to the carbon signal at 129.3 ppm and to the quaternary carbon at 145.6 ppm. Therefore, these two carbon signals are assigned to C5 and C1 respectively (H5 is assigned by HMQC). H4 and H6 are fixed by their connectivity in COSY with H3 and H5 (Fig. 3) and selective proton decoupling. Thus, this method allows phenyl-orthopalladated protons and carbons (inclusive quaternaries) to be assigned unambiguously.

The more significant bond lengths are collected in Table 1.

^{1}H NMR spectra of complexes **1a–c** show (Table 2) a sharp singlet at 2.31–2.33 ppm together with two weak singlets at ca. 2.28–2.30 and 2.36–2.39 ppm; also in complex **1a** there are two sharp peaks at 3.68 and 3.63 ppm assignable to *N*-methyl protons. These resonances are ascribed [2,3] to two geometrical isomers, anti and syn (the isomer ratio is 4:1, approximately). The acetate-bridged complexes **1a–c** adopt a boat conformation in which the cyclometalated ligands are nearly face-to-face and the ring protons are in the shielding region of the facing ligand. Thus, the ^{1}H NMR signals for these protons are shifted to lower frequencies, whereas this does not occur in the monomeric cyclometalated complexes.

^{1}H NMR spectra of complexes **4a–c** show unique signals for each proton of the corresponding ligands.

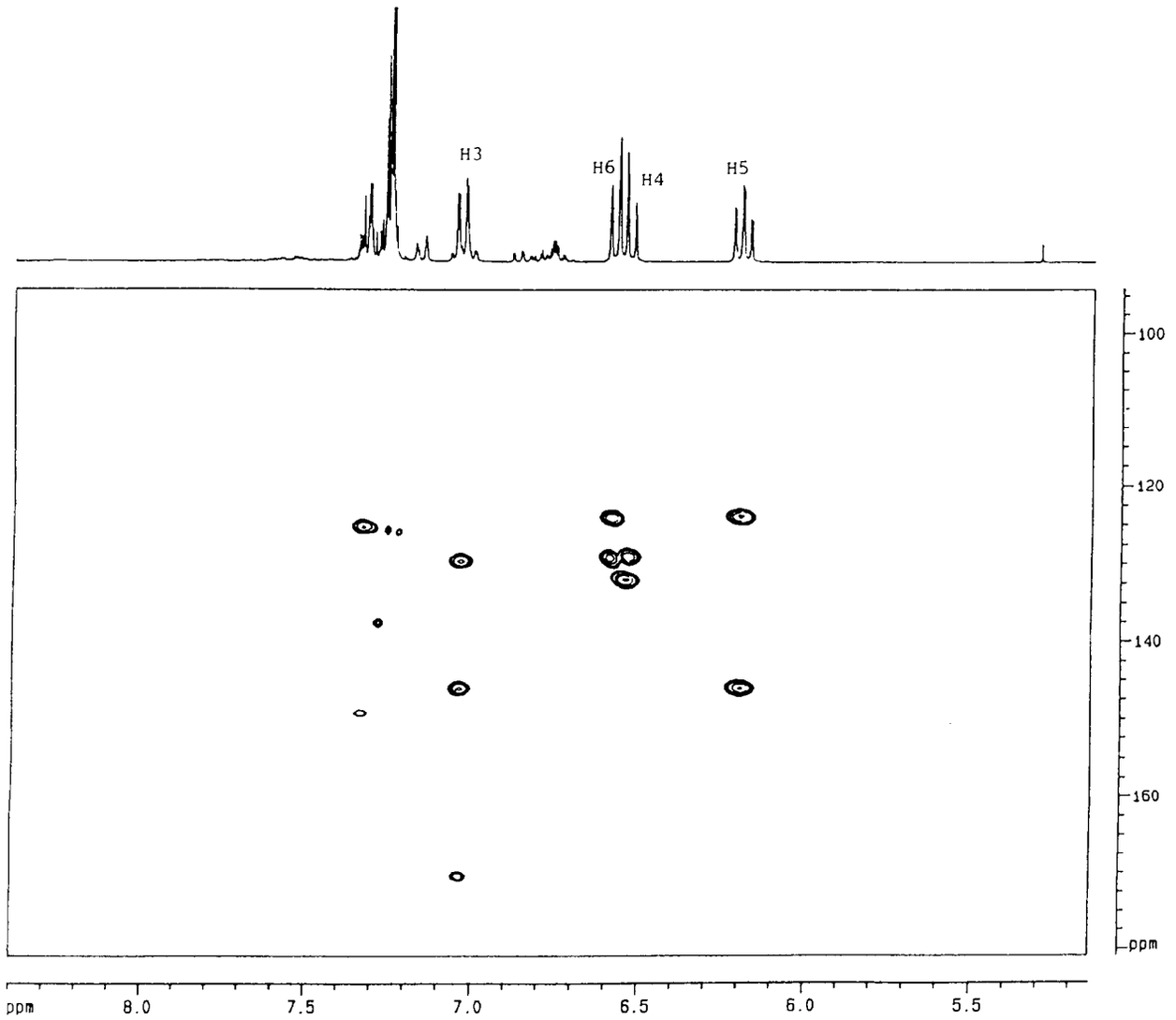

Fig. 2. HMBC experiment for **1c**.

Therefore, these complexes can only be those that show the SEt_2 trans at the nitrogen atom by the higher trans effect of the carbon atom.

The ^1H NMR spectra of **3a** and **3c** dimeric (it is not possible to obtain the **3b** spectrum due to its low solubility) and **4a–c** monomeric complexes are similar to each other but different to that observed in the folded acetate-bridged complexes. Shielding observed for H4 protons could be due primarily to the flow of charge from the electron-rich (d^8) palladium atom into the aromatic ring (π-back-bonding) [13]. The H3 protons, meta to the Pd–C bond, should be less affected by orthopalladation; however, they show a shielding that could be explained on the basis of orthopalladation together with changes in the ligand conformation [6].

Comparison of the ^{13}C NMR spectra of these orthopalladated complexes shows that there are no significant differences between them (Table 3). The C1 atom is strongly deshielded, probably due to the Pd–C back-bonding [5] since an increase in M–C bond order increases the deshielding term, σ^{para}, in Poeple's equation [14]. The down-field shift in carbon atoms C1′ and C2 must be attributed to orthopalladation. The variations observed in chemical shift of C3 carbons can be attributed to changes in conformation which occur within the ligand on orthopalladation [6]. The relatively large up-field shift of C4, para to the Pd–C bond and unaffected by steric interactions, clearly indicates the existence of Pd–C back-bonding [13]. The shielding of C3′ atoms observed in all the complexes, and also in monomeric cyclopalladated complexes of *N*-(4-methoxyphenyl)-α-benzoyl-benzylideneamine [5], is quite surprising and can only be understood by assuming that only steric effects are operating.

2.2. Crystal structure of complex 1c

The failed attempts to separate anti and syn isomers of the complexes **1a–c** by chromatography made us

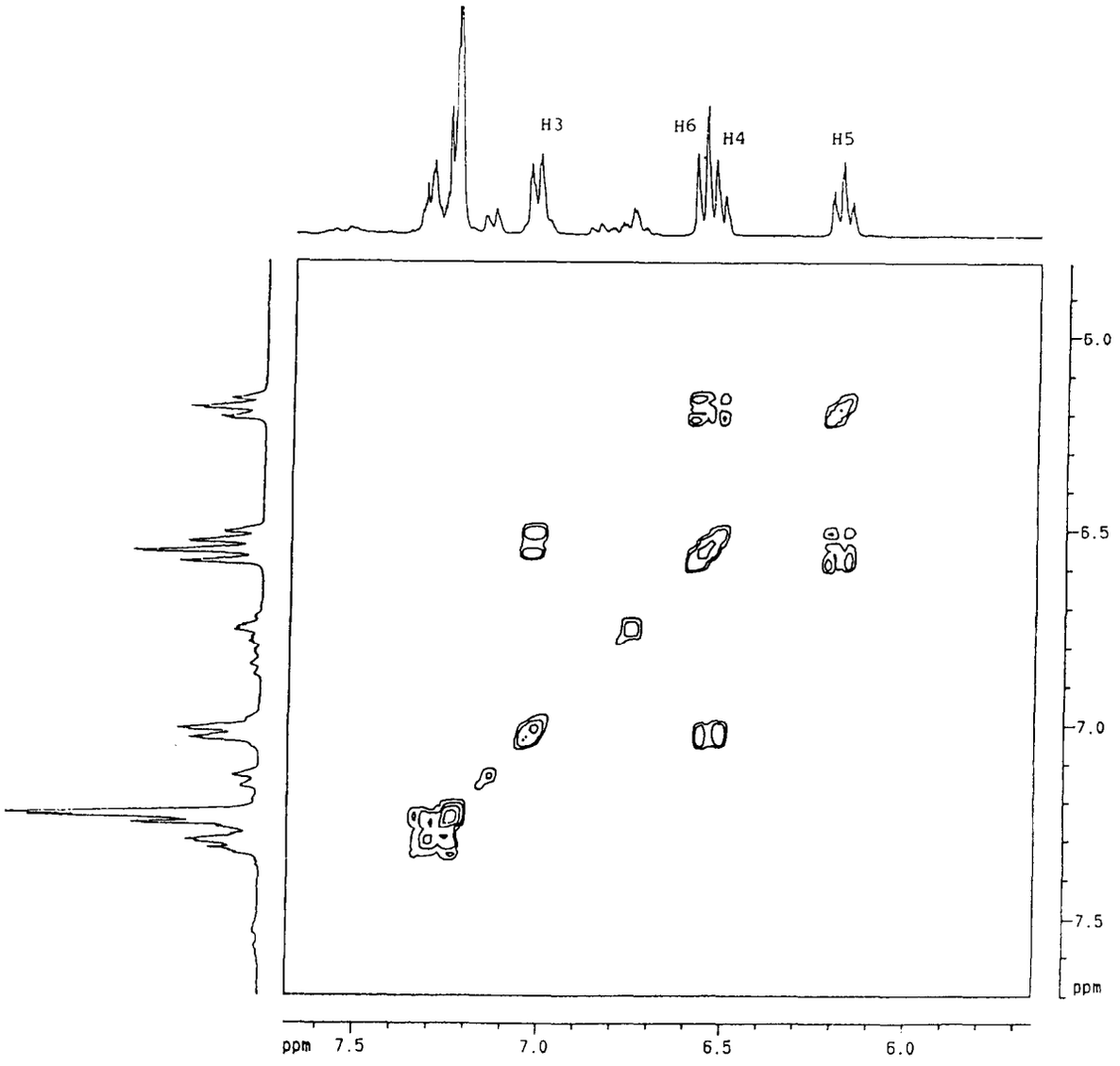

Fig. 3. COSY experiment for **1c**.

attempt the separation by crystallization. The crystallization affords the combined precipitation of orange (minority) and yellow (majority) crystals.

The X-ray structure analysis revealed that the two crystalline phases correspond to two polymorphic phases of the anti-isomer complex instead of the expected anti–syn isomers. The first one (orange crystals) is triclinic, $P\bar{1}$. While the other polymorph (yellow crystals) is monoclinic ($P2_1/n$, as has been previously described [7] for the related compounds $[(MeC_6H_3C_7H_4NO)Pd(\mu\text{-}OAc)]_2$ and $[(MeC_6H_3C_7H_4NS)\ Pd(\mu\text{-}OAc)]_2$).

A comparison of the molecular geometry in both phases revealed no significant difference between them. The molecule of the monoclinic phase is represented in Fig. 4. The more significant bond lengths are collected in Table 1.

A study of the distances NX–CX01, CX01–CX08, and CX08–CX09 in the cyclometalated ring of both polymorphic forms shows that all distances are in the range observed for compounds in which electronic delocalization in the cyclometalated ring is possible [4]. These results clearly suggest that this kind of cyclometalated ring shows some aromatic character, as was

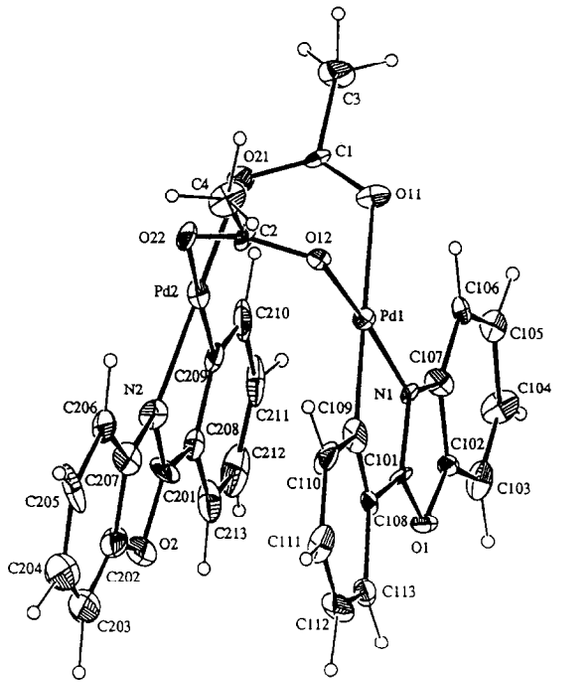

Fig. 4. The molecular structure of **1c**-yellow crystals (monoclinic phase) showing the atom numbering scheme.

Table 3
^{13}C NMR parameters (δ, ppm)

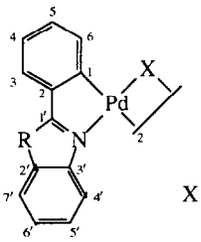

X =  (**1a–1c**), Br (**3a**, **3c**)

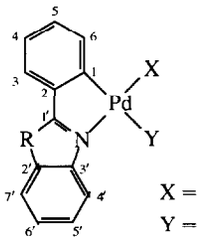

X = 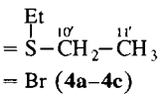
Y = Br (**4a–4c**)

	a [b]	**b** [b]	**c** [b]	**1a** [b,e]	**1b** [b,e]	**1c** [b,e]	**3a** [a]	**3c** [a]	**4a** [b]	**4b** [b]	**4c** [b]
C1	128.5	127.3	127.4	149.2	147.7	145.6	151.1	146.1	151.1	150.2	148.8
C2	130.0	130.8	127.0	134.4	138.7	137.2	139.5	140.4	136.2	141.4	131.6
C3	128.5	127.3	127.4	122.3	123.4	123.6	125.2	126.0	124.5	125.9	126.1
C4	129.3	128.4	128.7	121.3	123.5	123.7	124.3	124.9	124.9	125.7	125.5
C5	129.5	128.8	131.3	127.0	128.1	129.3	128.9	130.2	129.3	130.3	131.8
C6	129.3	128.4	128.7	132.4	131.1	131.6	134.8	139.1	133.4	132.4	132.5
C1′	153.6	167.8	162.8	157.1	175.7	170.0	157.5	175.0	159.0	178.9	172.0
C2′	136.4	133.4	142.0	134.1	130.2	132.6	135.4	130.9	134.7	130.6	139.1
C3′	142.8	153.9	150.6	139.2	149.5	148.8	139.5	150.1	141.1	151.5	149.4
C4′	119.6	123.0	119.8	117.2	121.6	117.6	123.6	121.1	121.7	125.3	121.4
C5′	122.6	126.0	124.9	123.3	126.6	125.4	123.3	127.5	123.9	127.3	126.0
C6′	122.2	125.0	124.4	122.7	124.9	124.8	123.3	123.4	123.4	125.6	125.5
C7′	109.5	121.4	110.4	108.9	121.3	111.0	111.1	123.4	108.8	121.5	110.7
N–CH_3	31.5			31.3 [c]					25.3		
				31.1 [d]							
C8′				24.8 [c]	24.9 [c]	24.6 [c]				31.6	32.7
				24.2 [d]	24.5 [d]	24.4 [d]					
C9′				181.4	181.5	181.8	32.2			13.6	13.5
C10′									32.1		
C11′									14.4		

[a] DMSO-d_6. [b] $CDCl_3$. [c] *anti* isomer. [d] *syn* isomer. [e] Other weak signals appeared corresponding to the *syn* isomer which are not possible to assign.

suggested in our work with complexes derived from benzoylbenzylideneamines [4].

3. Experimental section

Infrared spectra were recorded on a Perkin–Elmer 1650 spectrophotometer. NMR spectra were recorded with $CDCl_3$ or DMSO-d_6 solutions by using Bruker AMX-300. Elemental analyses were performed on a Perkin–Elmer 240B analyser.

Solvents were purified by the standard methods [15]. Palladium(II) acetate and chloride were purchased from Aldrich and Johnson-Matthey respectively. *N*-methyl-2-phenylbenzimidazole, 2-phenylbenzothiazole, 2-phenylbenzoxazole and diethylsulphide were purchased from Aldrich.

3.1. Synthesis of [{Pd(a–c)(μ-OAc)}$_2$] (1a–c)

Method 1. A mixture of equimolecular amounts of $Pd(OAc)_2$ and ligand in HOAc was heated at 60°C under N_2 for 6 h. Solvent was removed under vacuum and the residue extracted with CH_2Cl_2–H_2O 100 ml (1 : 1), dried over anhydrous Na_2SO_4 and filtered off. Solvent was eliminated on a rotary evaporator and the residue crystallized in CH_2Cl_2–hexane.

Method 2. To a suspension of **2a–c** (1 mmol) in acetone was added an equimolecular amount of AgOAc. After 12 h stirring the solution was filtered off and concentrated. When methanol was added, the solid obtained was recrystallized in CH_2Cl_2–hexane. Anal. Calc. for **1a**: C, 51.52; H, 3.76; N, 7.52. Found: C, 51.12; H, 3.51; N, 7.28%. M.p. 271–280°C dec.; yield method 1: 74.4% and 2: 80.1%; IR: υ_{max} 1572, 1412 cm^{-1}. Anal. Calc. for **1b**: C, 47.91; H, 2.95; N, 3.73. Found: C, 47.86; H, 2.69; N, 3.41%. M.p. 239–259°C dec.; yield method 1: 73.5% and 2: 75.7%; IR: υ_{max} 1566, 1414, 333 cm^{-1}. Anal. Calc. for **1c**: C, 50.04; H, 3.08; N, 3.89. Found: C, 49.91; H, 3.07; N, 3.80%. M.p. 197–199°C dec.; yield method 1: 60.0% and 2: 78.9%. IR: υ_{max} 1570, 1412, 339 cm^{-1}.

3.2. Synthesis of [{Pd(a–c)(μ-Cl)}$_2$] (2a–c)

Method 1. To a solution of **1a–c** (0.5 mmol) in 10 ml of acetone, was added a solution of NaCl (1 mmol) in 1 ml of water. The solid obtained after stirring for 12 h, at 20°C was filtered off, washed with water and acetone and dried in vacuo.

Method 2. To a solution of Li_2PdCl_4 prepared in situ from $PdCl_2$ (1 mmol) and LiCl (2 mmol) in 10 ml of methanol was added a solution of **2** (1 mmol) in 5 ml of methanol. The solution was heated at reflux with stirring for 24 h. The solid formed was filtered out, washed with methanol and dried in vacuo. Anal. Calc. for **2a**: C, 48.12; H, 3.15; N, 8.02. Found: C, 48.12; H, 3.12; N, 7.82%. M.p. > 300°C; yield method 1: 77.5%; IR: υ_{max} 348, 327, 280 cm^{-1}. Anal. Calc. for **2b**: C, 44.30; H, 2.29; N, 3.97. Found: C, 44.12; H, 2.28; N, 3.66%. M.p. 245–264°C dec.; yield method 1: 74.7% and 2: 70.2%; IR: υ_{max} 336, 312, 294 cm^{-1} Anal. Calc. for **2c**: C, 46.41; H, 2.38; N, 4.16. Found: C, 46.39; H, 2.24; N, 4.14%. M.p. 272–281°C dec.; yield method 1: 74.4% and 2: 80.1%; IR: υ_{max} 342, 333, 279 cm^{-1}.

3.3. Synthesis of [{Pd(a–c)(μ-Br)}$_2$] (3a–c)

To a solution of **1a–c** (0.5 mmol) in 10 ml of acetone was added a solution of LiBr (1 mmol) in 1 ml of water. The solid obtained after stirring for 12 h at 20°C was filtered off, washed with water and acetone and dried in vacuo. Anal. Calc. for **3a**: C, 42.73; H, 2.81; N, 7.11. Found: C, 42.55; H, 2.65; N, 7.05%. M.p. > 300°C; yield 84.1%; IR: υ_{max} 342 cm^{-1}. Anal. Calc. for **3b**: C, 39.37; H, 2.03; N, 3.53. Found: C, 39.76; H, 1.96; N, 3.59%. M.p. 293–298°C; yield 76.2%; IR: υ_{max} 346 cm^{-1}. Anal. Calc. for **3c**: C, 41.03; H, 2.12; N, 3.68. Found: C, 40.99; H, 1.89; N, 3.64%. M.p. > 300°C; yield 91.3%; IR: υ_{max} 330 cm^{-1}.

3.4. Synthesis of [Pd(a–c)Br(SEt$_2$)] (4a–c)

To a suspension of complex **3a–c** (0.5 mmol) in CH_2Cl_2 was added SEt_2 (2 mmol). The yellow solution obtained after stirring for 12 h at 20°C was filtered off and concentrated on a rotary evaporator. Addition of diethyl ether gave a solid, which was filtered off, washed with diethyl ether, and dried in vacuo. Anal. Calc. for **4a**: C, 45.59; H, 4.37; N, 5.78. Found: C, 45.99; H, 4.33; N, 5.72%. M.p. 238–240°C dec.; yield 88.9%; IR: υ_{max} 341 cm^{-1}. Anal. Calc. for **4b**: C, 41.95; H, 3.73; N, 2.88. Found: C, 41.82; H, 3.69; N, 2.87%. M.p. 200–205°C dec.; yield 98.2%; IR: υ_{max} 328 cm^{-1}. Anal. Calc. for **4c**: C, 43.38; H, 3.85; N, 2.97. Found: C, 43.05; H, 3.61; N, 2.88%. M.p. 230–237°C dec.; yield 98.0%; IR: υ_{max} 320 cm^{-1}.

3.5. Structural analysis

The recrystallization of the related complex **1c** from CH_2Cl_2–hexane gave rise to the appearance of two different types of crystal. Both, with parallelepiped aspect, presented well-defined characteristic colours: orange and yellow.

3.5.1. Crystal data for complex 1c-orange crystals

$Pd_2C_{30}H_{22}O_6N_2$. M_r = 719.314, triclinic ($P\bar{1}$). a = 12.578 (1) Å, b = 13.134 (2) Å, c = 17.615 (2) Å, α = 103.47 (1)°, β = 97.57 (1)°, γ = 104.15 (1)°, V =

2688.6 (5) Å^3, $Z = 4$. $D_{calc} = 1.777$ g cm^{-3}. $F(000) = 1424$, $\mu = 13.660$ cm^{-1}. An orange crystal ($0.20 \times 0.18 \times 0.15$ mm^3) was used to collect data on a PW-1100 diffractometer using graphite monochromated Mo Kα radiation. A total of 4523 independent reflections were measured. Of these 4133 with $I \geq 3\sigma(I)$ were considered as observed.

The structure was solved by heavy-atoms methods, and refined with anisotropic parameters for all non-H atoms. The H atoms were fixed at the calculated positions. No absorption corrections were applied. Atomic scattering factors for neutral atoms and anomalous dispersion factors for Pd from the *International Tables for X-ray Crystallography* were used. A total of 721 parameters were varied by using units weights. The final $R = 0.045$, $Rw = 0.049$.

3.5.2. Crystal data for complex **1c***-yellow crystals*

$Pd_2C_{30}H_{22}O_6N_2$ $M_r = 719.314$, monoclinic ($P2_1/n$). $a = 9.450$ (2) Å, $b = 23.423$ (6) Å, $c = 12.661$ (2), $\beta = 109.02$ (2), $V = 2650$ (1) Å^3. $Z = 4$. $D_{calc} = 1.8032$ g cm^{-3}; $F(000) = 1424$, $\mu = 13.861$ cm^{-1}. A yellow crystal ($0.15 \times 0.25 \times 0.10$ mm^3) was used to collect data on a CAD-4 Enraf–Nonius diffractometer using graphite monochromated Mo Kα radiation. At room temperature, the intensity was only observed up to 15°. So, the data were collected at 200 K. A total of 6358 independent reflections were measured. Of these, 1299 with $I \geq 2\sigma(I)$ were considered as observed. The structure was solved by heavy atom methods and refined with anisotropic parameters for all non-H atoms. The H atoms were fixed at the calculated positions. A total of 361 parameters were varied by using units weights. As in the first case, atomic scattering factors for neutral atoms and anomalous dispersion factors for Pd from the *International Tables for X-ray Crystallography* were used. The final R = 0.054 and Rw = 0.065.

All calculations for complex **1c**-orange and complex **1c**-yellow were performed by using the XRAY 80 [16] and DIRDIF [17].

4. Supplementary material available

Atomic coordinates, listings of anisotropic thermal parameters and tables of observed and calculated structure factors for complex **1c**-orange (21 pages) and **1c**-yellow (26 pages) are available.

Acknowledgment

We wish to thank Jonhson Matthey Chem-Ltd for their generous gift of K_2PdCl_4 and $PdCl_2$. This work has been supported by grant no SAF 93-1122. We also thank the assistance in NMR of Dr. R. Ferrito, in XRD of Dr. A. Vegas and the useful discussions of Dr. P. Amo.

References

[1] (a) A.D. Ryabov, *Chem. Rev.*, *90* (1990) 403. (b) D.W. Evans, G.R. Baker and G.R. Newkome, *Coord. Chem. Rev.*, *93* (1989) 155. (c) I. Omae, *Coord. Chem. Rev.*, *83* (1988) 137.

[2] K. Hiraki, Y. Fuchita, H. Nakaya and S. Takakura, *Bull. Chem. Soc. Jpn.*, *52* (1979) 2531.

[3] G. Balavoine, J.C. Clinet, P. Zerbib and K. Boubekeur, *J. Organomet. Chem.*, *389* (1990) 259.

[4] C. Navarro-Ranninger, I. López-Solera, A. Alvarez-Valdés, J.H. Rodríguez-Ramos, J.R. Masaguer, J.L. García -Ruano and X. Solans, *Organometallics*, *12* (1993) 4104.

[5] J.L. García-Ruano, I. López-Solera, J.R. Masaguer, M.A. Monge, C. Navarro-Ranninger and J.H. Rodríguez -Ramos, *J. Organomet. Chem.*, *476* (1994) 111.

[6] P.J. Steel and G.B. Caygill, *J. Organomet. Chem.*, *327* (1987) 101.

[7] M.R. Churchill, H.J. Wasserman and G. Young, *Inorg. Chem.*, *19* (1980) 762.

[8] (a) A. Bax, R.H. Griffey and B.L. Hawhins, *J. Magn. Reson.*, *55* (1983) 301. (b) M.F. Summers, L.G.. Marzilli and A. Bax, *J. Am. Chem. Soc.*, *108* (1986) 4285. (c) A. Bax and S. Subramanian, *J. Magn. Reson.*, *67* (1986) 565.

[9] A. Bax and M.F. Summers, *J. Am. Chem. Soc.*, *108* (1986) 2093.

[10] K. Nakamoto, *IR and Raman Spectra of Inorganic and Coordination Compounds*, Wiley–Interscience, 4th edn., 1986.

[11] B. Crociani, T. Boshi, R. Pieetropaolo and U. Belluco, *J. Chem. Soc. A*, (1970) 531.

[12] D.J. Cárdenas, A. Echavarren and A. Vegas, *Organometallics*, *13* (1994) 882.

[13] M.A. Gutiérrez, G.R. Newkome and J. Selbin, *J. Organomet. Chem.*, *202* (1980) 341.

[14] B. Crociani, F. Di Bianca and A. Giovenco, *Organomet. Chem.*, *251* (1983) 393.

[15] D.D. Perrin, W.L.F. Armarego and D.R. Perrin, *Purification of Laboratory Chemicals*, Pergamon, Oxford, 2nd edn., 1980.

[16] J.M. Steewarts (ed.) *The* XRAY *System of Crystallographic Programs*, (version of 1980) *Tech. Rep. TR-446*, 1978 (Computer Science Center, University of Maryland, College Park, MD, USA).

[17] P. Beurskens, W.P. Bosman, H.M. Doesburg, R.O. Gould, T.E.M. Van den Hark, P.A.J. Prick, J.H. Noordij, V. Parthasarati, H.J. Bruins-Slot, R.C. Haltiwanger and J.M.M. Smits, DIRDIF *System*. Crystallography Laboratory, Toernooivel, Nijmegen, Netherlands, 1984.